
Universal Value Density Estimation for Imitation Learning and Goal-Conditioned Reinforcement Learning

Yannick Schroecker¹ Charles Isbell¹

Abstract

This work considers two distinct settings: imitation learning and goal-conditioned reinforcement learning. In either case, effective solutions require the agent to reliably reach a specified state (a goal), or set of states (a demonstration). Drawing a connection between probabilistic long-term dynamics and the desired value function, this work introduces an approach which utilizes recent advances in density estimation to effectively learn to reach a given state. As our first contribution, we use this approach for goal-conditioned reinforcement learning and show that it is both efficient and does not suffer from hindsight bias in stochastic domains. As our second contribution, we extend the approach to imitation learning and show that it achieves state-of-the-art demonstration sample-efficiency on standard benchmark tasks.

1. Introduction

Effective imitation learning relies on information encoded in the demonstration states. In the past, successful and sample-efficient approaches have attempted to match the distribution of the demonstrated states (Ziebart et al., 2008; Ho and Ermon, 2016; Schroecker et al., 2019), reach any state that is part of the demonstrations (Wang et al., 2019; Reddy et al., 2019), or track a reference trajectory to reproduce a specific sequence of states (Peng et al., 2018; Aytar et al., 2018; Pathak et al., 2018). Without explicitly trying to reproduce demonstrated states, imitation learning suffers from the problem of accumulating errors (Ross et al., 2011) and requires a larger amount of demonstration data to accurately reproduce the expert’s behavior. Furthermore, without reasoning about how to reach desired states, the agent will be unable to learn from observation alone. The question of how to reach desired target states has also been separately considered as part of another field of study:

goal-conditioned reinforcement learning. Goal-conditioned reinforcement learning aims to train flexible agents that can solve multiple variations of a given task by parameterizing it with a goal. Often, this goal takes the form of a state or desired observation that the agent has to visit or achieve in the most optimal way. In this case, the task becomes highly similar to the setting of imitation learning: where goal-conditioned reinforcement learning trains the agent to reach a single given goal state, common approaches to efficient imitation learning teach the agent to reach multiple given goal states, i.e. to match a distribution or sequence of demonstrated states.

Despite significant achievements in the field (Schaul et al., 2015; Andrychowicz et al., 2017; Nair et al., 2018; Sahni et al., 2019), learning to achieve arbitrary goals remains an extremely difficult challenge. In the absence of a suitably shaped reward function, the signal given to the agent can be as little as a constant reward if the goal is achieved and 0 otherwise. Such a reward function is sparse and difficult to learn from, a problem that is only exacerbated when the task is to achieve any arbitrary goal. Hindsight Experience Replay (HER) (Andrychowicz et al., 2017) introduces the concept of hindsight samples as an effective heuristic to tackle this problem. Hindsight sampling selects transitions from past experience but artificially changes the goal during the learning process to pretend that the agent intended to reach the state that it actually observed later in the rollout. This way, the agent will frequently observe a reward and receive a comparatively dense learning signal. HER provides remarkable speed-ups and is capable of solving a variety of sparse, goal-conditioned RL problems; however, the approach cannot be applied to all domains as it suffers from hindsight bias. By changing the goal in hindsight, the agent implicitly discards unsuccessful attempts. As a result, if an action has a large failure rate and leads the agent to succeed in only a small fraction of all attempts, the value of the action will be dramatically overestimated.

Addressing problems in goal-conditioned reinforcement learning and in imitation learning, our work makes two central contributions:

1. We introduce an alternative and unbiased approach to utilize hindsight samples, enabling sample-efficient

¹College of Computing, Georgia Institute of Technology. Correspondence to: Yannick Schroecker <yannickschroecker@gatech.edu>.

goal-conditioned reinforcement learning in domains that prior methods cannot solve.

2. We introduce an imitation learning method based on this approach and show that it outperforms the current state-of-the-art in demonstration sample-efficiency on common benchmark tasks.

Utilizing hindsight samples alone to achieve unbiased goal-conditioned reinforcement learning in the general case is impossible: if we never sample negative transitions, we cannot train the agent to accurately assess the risks of such transitions; however, the most common formulation and a useful special case assigns a positive reward to states in which the goal has been achieved and provides a reward of 0 otherwise¹ (with an additional, optional term handling action cost). We observe that the long-term expected reward in such a scenario is directly proportional to the discounted likelihood of achieving this goal. We propose the term ‘‘Value Density’’ to refer to a special case of a value function that is also a valid representation of this likelihood. We furthermore observe that hindsight samples provide us with exactly the state-action and achieved goal triplets that are required for estimating the density of achieved goals. This gives rise to value density estimation: using a modern density estimator (Dinh et al., 2016), we utilize hindsight samples to directly estimate the value function. Combined with regular temporal difference learning updates, this approach allows us to estimate the value function for each goal in a way that is sample-efficient, unbiased and low-variance. We will explore this approach in detail in Section 4.

To extend this approach to imitation learning, we teach the agent to reproduce the distribution of states that the expert teacher has demonstrated to the agent. This encourages the agent to stay close to demonstration states and prevents errors from accumulating, a problem which is largely responsible for inefficiencies in imitation learning approaches. Errors accumulate when the agent deviates from demonstrations and has to make decisions in states that are unlike any it has seen as part of the demonstration set. Sampling demonstration-states as goals, we can utilize the same approach to teach the agent to stay near the demonstrated states. To ensure that the agent attempts to visit all states equally often, i.e. to ensure that the agent matches the expert’s state-distribution rather than sticking to a subset of demonstrated states, we have to pick demonstration states as goals with higher probability if the state is unlikely to be visited by the agent and vice versa. To this end, we maintain a model of the agent’s state-distribution as well. We describe this approach in detail in Section 5.

¹This scenario is also the primary focus of the original Hindsight Experience Replay experiments

2. Background

2.1. Markov Decision Processes

Markov Decision Processes (MDPs) are an essential formalism to describe sequential decision making problems such as reinforcement learning and imitation learning. Here, we briefly lay out notation while referring the reader to Puterman (2014) for a detailed review. MDPs define a set of states \mathbb{S} , a set of actions \mathbb{A} , a distribution of initial states $d_0(s)$, Markovian transition dynamics defining the probability (density) of transitioning from state s to s' when taking action a as $p(s'|s, a)$, and a reward function $r(s, a)$. In reinforcement learning, we commonly wish to find a parametric stationary policy $\mu_\theta : \mathbb{S} \rightarrow \mathbb{A}$. Here, we write the policy as a deterministic function as we will utilize deterministic policy gradients, but all findings hold for stochastic policies as well. An optimal policy is one which maximizes the long-term discounted reward $J_\gamma^r(\theta) = E[\sum_{t=0}^{\infty} \gamma^t r(s_t, a_t) | s_0 \sim d_0, \mu_\theta]$ given a discount factor γ or, sometimes, the average reward $J^r(\theta) = \int d^{\pi_\theta}(s) r(s, \mu_\theta(s)) ds, a$, where the stationary state distribution $d^\mu(s)$ and the stationary state-action distribution $\rho^\mu(s, a)$ are uniquely induced by μ under mild ergodicity assumptions. A useful concept to this end is the value function $V^\mu(s) = E[\sum_{t=0}^{\infty} \gamma^t r(s_t, a_t) | s_0 = s, \mu]$ or Q function $Q^\mu(s, a) = E[\sum_{t=0}^{\infty} \gamma^t r(s_t, a_t) | s_0 = s, a_0 = a, \mu]$ which can be used to estimate the policy gradient $\nabla_\theta J_\gamma(\theta)$ (e.g. Sutton et al., 1999; Silver et al., 2014). Finally, we define as $p_\mu(s, a \xrightarrow{t} s')$ the probability of transitioning from state s to s' after t steps when taking action a in state s and following policy μ .

2.2. Goal-conditioned Reinforcement Learning

Goal-conditioned Reinforcement Learning aims to teach an agent to solve multiple variations of a task, identified by a goal vector g . Conditioned on the goal, the reward function $r^g(s, a)$ describes all possible instantiations of the task. To solve each possible variation, the agent learns a representation of a goal-conditioned policy, which we write as $\mu_\theta^g(s)$. Based on the goal-conditioned reward and policy, we can write down a generalized definition of the value function. Note that the policy and the reward can be conditioned on different goals:

$$V_{r^g}^{\mu^g}(s) = E\left[\sum_{t=0}^{\infty} \gamma^t r^g(s_t, a_t) | s_0 = s, \mu^g\right] \quad (1)$$

To solve such tasks, Schaul et al. (2015) introduce the concept of a Universal Value Function Approximator (UVFA), a learned model $V_\omega(s; g)$ approximating $V_{r^g}^{\mu^g}(s)$, i.e. all value functions where the policy and reward are conditioned on the same goal. For the purposes of this work, we also consider models which generalize over different value-functions, but consider a fixed, specific policy. To distinguish such models

visually, we write $\tilde{V}_\omega(s; g)$ to refer to models which approximate $V_{r_g}^\mu(s)$ for a given μ . Where V_ω represents how good the agent is at achieving any goal if it tries to achieve it, \tilde{V}_ω models how good a specific policy is, if the task were to achieve the given goal.

Schaul et al. (2015) show that UVFAs can be trained via regular temporal difference learning with randomly sampled goals. This allows the agent to learn a goal-conditioned policy using regular policy gradient updates; however, sampling goals at random requires the reward signal to be sufficiently dense. A common use-case for goal-conditioned reinforcement learning involves solving problems with a sparse reward, for example an indicator function that tells the agent whether a goal has been achieved. In this case, the agent rarely observes a non-zero reward while training the UVFA. Hindsight updates (HER) (Andrychowicz et al., 2017) are a straight-forward solution, changing goals recorded in a replay memory based on what the agent has actually achieved in hindsight. While the approach is intuitive, it is also biased. We will explore the significance of this further in Section 3.1 where we also introduce an alternative solution that is both efficient and unbiased.

2.3. Imitation Learning

Imitation learning (IL) teaches agents to act given demonstrated example behavior. While the MDP formalism can still be used in this scenario, we no longer have a pre-defined reward function specifying the objective. Instead, we are given a sequence of expert state-action pairs. The goal of imitation learning is to learn a policy μ_θ that is equivalent to the expert’s policy μ^* which generated the demonstrated states and actions. This problem is underspecified and different formalizations have been proposed to achieve this goal. The simplest solution to IL is known as Behavioral Cloning (BC) (Pomerleau, 1989) and treats the problem as a supervised learning problem. Using demonstrated states as sample inputs and demonstrated actions as target outputs, a policy can be trained easily without requiring further knowledge of, or interaction with, the environment. While this approach can work remarkably well, it is known to be suboptimal as a standard assumption of supervised learning is violated: predictions made by the agents affect future inputs to the policy (Ross et al., 2011). By learning about the environment dynamics and explicitly trying to reproduce future demonstrated states, the agent is able to learn more robust policies from small amounts of demonstration data.

A common and effective formalism is to reason explicitly about matching the distribution of state-action pairs that the agent will see to that of the expert. By learning from interaction with the environment and employing sequential reasoning, approaches such as maximum entropy IRL (Ziebart et al., 2008), adversarial IRL (Fu et al., 2018),

GPRIL (Schroecker et al., 2019) or Generative Adversarial Imitation Learning (GAIL) (Ho and Ermon, 2016) lead the agent to reproduce the expert’s observations as well as the expert’s actions. By drawing a connection to goal-conditioned reinforcement learning, we introduce a novel approach to match the expert’s state-action distribution and will show that it outperforms the current state-of-the-art on common benchmark task.

2.4. Normalizing Flows

Recent years have seen rapid advances in the field of deep generative modeling. While much of the field has focused on generating representative samples (Kingma and Welling, 2014; Goodfellow et al., 2014), methods such as autoregressive models (van den Oord et al., 2016; van den Oord et al., 2016) and normalizing flows (van den Oord et al., 2017; Dinh et al., 2016) have demonstrated the ability to learn an explicit representation of complex density functions. In this work, we require the ability to estimate highly non-linear Value Density functions and utilize a simplified version of RealNVP (Dinh et al., 2016) for this purpose. As a Normalizing Flow, RealNVPs consist of a series of learned, invertible transformations which transform samples $z \in \mathbb{R}^N$ from one distribution p_z to samples $x \in \mathbb{R}^N$ from another distribution p_x . Chaining multiple bijective transformations allows the model to transform simple density functions, such as a unit Gaussian, to represent complex distributions such as images (in the original paper) or the agent’s state (in this work). Normalizing flows represent the density function explicitly and in a differentiable way, such that the model can be trained via maximum likelihood optimization. To ensure that the density function and its gradient are tractable, special care has to be taken in picking the right bijective transformation. RealNVP utilizes affine transformations where half of the input features are scaled and shifted, with scale and shift parameters predicted based on the other half. While the original work defines a specific autoregressive order to model images effectively, we use a simplified version of RealNVP in this paper to model non-image data and pick the autoregressive order at random.

3. Universal Value Density Estimation

3.1. Addressing Hindsight Bias

To teach the agent to reach desired states, either for the purposes of goal-conditioned reinforcement learning or for imitation learning, we first consider the question of learning approximations of the goal-conditioned value-functions \tilde{V}_ω or V_ω , using fixed or goal-conditioned policies respectively. Either requires us to address the challenge of learning from sparse rewards. Andrychowicz et al. (2017) train UVFAs efficiently by replacing the original goal with the achieved goal. Allowing the agent to learn from failures, HER pro-

Algorithm 1 Universal Value Density Estimation (UVD)

```

1: function UVD
2:   for  $i \leftarrow 0..#\text{Iterations}$  do
3:     Fill replay buffer with experience
4:     for  $s, a, \bar{g}$  sampled from short replay buffer do
5:       Sample time offsets  $t \sim \text{Geom}(1 - \gamma)$ 
6:       Sample achieved goals  $g$   $t$  steps ahead of  $s$ 
7:       Update  $F_\Phi$  with  $-\nabla_\Phi \log F_\Phi(g|s, a, \bar{g})$ 
8:     for  $s, a, s', \bar{g}$  sampled from long replay buffer do
9:        $\bar{Q} \leftarrow \max \left( F_\Phi(\bar{g}|s', \mu_\theta^\bar{g}(s'), \bar{g}), Q_{\bar{\omega}}(s', \mu_\theta^\bar{g}(s')) \right)$ 
10:      Update  $Q_\omega$  with  $\nabla_\omega (r^{\bar{g}}(s, a) + \gamma \bar{Q} - Q_\omega(s, a; \bar{g}))^2$ 
11:      Update  $\mu_\theta^\bar{g}$  with  $\nabla_a Q_\omega(s, a; \bar{g}) \Big|_{a=\mu_\theta^\bar{g}(s)} \nabla_\theta \mu_\theta^\bar{g}(s)$ 

```

of time-steps apart, leading to updates which suffer from extremely high variance. Temporal difference learning uses bootstrapping to reduce the variance of the regression gradient and to handle such large time-horizons. In practice, temporal difference learning is likely to underestimate the true value as it may never observe a reward³. Density estimation does not suffer from a sparse learning signal, but in practice we have to limit the time-horizon to limit variance. The result is that the density estimator will underestimate the value as well.

Here, we propose to combine both estimators to get the best of both approaches. There are a variety of ways in which the two estimators can be integrated. Fujimoto et al. (2018) combine two estimators to combat overestimation by choosing the smaller value in the computation of the temporal difference target. In this work, we follow a similar approach and combat underestimation by choosing the larger of the two estimators to compute the temporal difference target. The temporal difference loss is then given by

$$L(\omega) := \left(r^g(s, a) + \gamma \bar{Q} - \tilde{Q}_\omega(s, a; g) \right)^2, \quad (4)$$

$$\bar{Q} := \max \left(\tilde{Q}_\omega(s, a; g), F_\Phi(g|s, a) \right), \quad (5)$$

where $F_\Phi(g|s, a)$ is a learned estimate of the density defined in Eq. 3.

4. Goal-conditioned Reinforcement Learning

Using the general principle introduced in the previous section, we now introduce Universal Value Density Estimation (UVD) to address the problem of goal-conditioned reinforcement learning. Using Eq. 4, we can efficiently estimate the Q-function corresponding to a goal-conditioned reward function; however, in goal-conditioned reinforcement learning, the policy needs to be conditioned on the goal as well. Using a goal-conditioned policy in Eq. 3, we can write

³if the environment is continuous and stochastic and the reward is as defined above, we can assume that the agent never observes a reward

Algorithm 2 Value Density Imitation (VDI)

```

1: function VDI
2:   for  $i \leftarrow 0..#\text{Iterations}$  do
3:     Fill replay buffer with experience
4:     for  $s, a$  sampled from short replay buffer do
5:       Sample time offsets  $t \sim \text{Geom}(1 - \gamma)$ 
6:       Sample target states  $\bar{s}$   $t$  steps ahead of  $s$ 
7:       Update  $F_\Phi$  with  $-\nabla_\Phi \log F_\Phi(\bar{s}|s, a)$ 
8:       Update  $d_\Phi$  with  $-\nabla_\Phi \log d_\Phi(s)$ 
9:     for  $s, a, s'$  sampled from long replay buffer do
10:      Sample  $\bar{s}$  uniformly from expert data
11:       $\bar{Q} \leftarrow \max \left( F_\omega(\bar{s}|s, a), \gamma \tilde{Q}_\omega(s', \mu_\theta(s')) \right)$ 
12:      Update  $\tilde{Q}_\omega$  with  $\nabla_\omega \left( \bar{Q} - \tilde{Q}_\omega(s, a; \bar{s}) \right)^2$ 
13:    for  $s, a$  from long replay buffer do
14:      Sample  $\bar{s}$  from expert data with  $p = \frac{1}{d_\Phi(\bar{s})}$ 
15:      Update  $\mu_\theta$  with  $\nabla_a \tilde{Q}_\omega(s, a; \bar{s}) \Big|_{a=\mu_\theta(s)} \nabla_\theta \mu_\theta(s)$ 

```

down a corresponding equivalence to a predictive long-term generative model:

$$F_\gamma^{\mu_\theta^\bar{g}}(g|s, a) := Q_{r^g}^{\mu_\theta^\bar{g}}(s, a) \quad (6)$$

Here, $F_\gamma^{\mu_\theta^\bar{g}}(g|s, a)$ corresponds to the distribution of goals g that the agent will reach when it starts in state s , takes action a and then tries to reach the goal \bar{g} . As before, we can easily train a model to represent this distribution via density estimation. In this case, the model has to be conditioned on the intended goal \bar{g} as well and takes the form $F_\Phi(g|s, a, \bar{g})$. Using this density estimate, we can alter the temporal difference target in Eq. 4 to efficiently train a UVFA:

$$\bar{Q} := \max(Q_{\bar{\omega}}(s, a; g), F_\Phi(g|s, a, \bar{g})) \quad (7)$$

We can now write down an iterative algorithm for goal-conditioned reinforcement learning that is able to handle sparse reward signals while also addressing the problem of hindsight bias. First, the agent collects experience with a randomly sampled intended goal. By interacting with the environment, the agent observes future achieved goals and models their distribution conditioned on the intended goal and the current state-action pair. Next, the agent uses the learned density estimator to update the Q-function as in Eq. 7. Finally, the agent updates the goal-conditioned policy using the learned UVFA to estimate the policy gradient. The approach is described in more detail in Algorithm 1, while implementation details are discussed in Appendix A.

5. Imitation Learning

We now turn our attention to the problem of sample-efficient imitation learning. We wish to train the agent to imitate an expert's policy using only a few demonstration samples from the expert. Different formulations exist to solve this

problem (see Section 2.3), but the formulation which has arguably been the most promising in the recent past has been to train the agent to explicitly match the expert’s state-action distribution or occupancy measure (Ziebart et al., 2008; Ho and Ermon, 2016). Our next step is therefore to extend our findings from the previous section to state-action or state distribution matching.

Similar to Schroecker and Isbell (2017); Schroecker et al. (2019), we propose a maximum-likelihood approach to the distribution-matching problem. Central to this approach is the estimation of the state-distribution gradient $\nabla_{\theta} \log d^{\mu_{\theta}}(\bar{s})$. By itself, following the state-distribution gradient leads the agent to reproduce the expert’s state-distribution which is ambiguous and may admit multiple solutions. In practice, however, state-distribution matching can often be an effective approach to imitation learning and is optimal if the expert’s behavior can be uniquely described using a reward-function that depends only on the current state. We will evaluate state-distribution matching as imitation from observation in Section 6.2. To use the gradient estimate for state-action distribution matching, it is possible to combine it with the behavioral cloning gradient as $\nabla_{\theta} \log \rho^{\pi_{\theta}}(\bar{s}, \bar{a}) = \nabla_{\theta} \log \pi_{\theta}(\bar{a}|\bar{s}) + \nabla_{\theta} \log d^{\pi_{\theta}}(\bar{s})$, where we assume a stochastic policy π_{θ} in place of a deterministic one. We found, however, that the behavioral cloning gradient can dominate a noisy estimate of the state-distribution gradient and lead to overfitting. Instead, we propose to augment the state to include the previous action that lead to the state. This approach attempts to match the joint distribution of action and next state which implies the state-action-distribution based on environment dynamics.

If applied to a single state, following the state-distribution gradient teaches the agent to go to that state. It is thus no surprise that it can be shown to be equivalent to the policy gradient for the right goal-conditioned reward function (also see Schroecker et al., 2019). Specifically, the state-distribution gradient is equivalent to the weighted policy gradient in the average-reward setting (using $r^{\bar{s}}(s, a) = \delta_{s, \bar{s}}$). We have:

$$\begin{aligned} \nabla_{\theta} \log d^{\mu_{\theta}}(\bar{s}) &= \frac{\nabla_{\theta} d^{\mu_{\theta}}(\bar{s})}{d^{\mu_{\theta}}(\bar{s})} \\ &= \nabla_{\theta} \frac{\int d^{\mu_{\theta}}(s) \delta_{s, \bar{s}} ds}{d^{\mu_{\theta}}(\bar{s})} = \frac{\nabla_{\theta} J^{r^{\bar{s}}}(\theta)}{d^{\mu_{\theta}}(\bar{s})} \end{aligned} \quad (8)$$

Intuitively, the policy gradient leads the agent toward a demonstration state \bar{s} , while the weight ensures that all demonstration states are visited with equal probability. This gives rise to Value Density Imitation Learning (see Alg. 2):

1. Using self-supervised roll-outs, learn the goal-conditioned Q function as in section 3.
2. Using same roll-outs, train an unconditional density estimator to model the agent’s state-distribution: $d_{\omega}(s)$.

3. Sample demonstration states with probability proportional to $\frac{1}{d_{\omega}(\bar{s})}$.
4. Use the learned Q function, conditioned on the sampled demonstration states, to estimate the policy gradient.

6. Experiments

6.1. Goal-Conditioned Reinforcement Learning

We first evaluate UVD on a suite of simulated manipulation tasks involving a Fetch robot arm. This suite has been developed by Andrychowicz et al. (2017) to show the strengths of hindsight experience replay. As the simulation is fully deterministic, the effects of hindsight bias don’t play a role in these environments. Our goal here is therefore to show UVD to solve the unmodified tasks as efficiently as HER while outperforming it on a stochastic variation of the domain. We compare all methods using the same hyper-parameters, which can be found in Appendix C.

The first domain in the suite, *FetchPush*, requires the robot arm to learn to push an object to any given target location. The reward signal is sparse as the agent is given a non-zero reward only if the object reaches the desired location. In Figure 2a, we can see that TD3 with HER and TD3 with UVD perform similarly. Contrary to the original findings by Andrychowicz et al. (2017), we also find unmodified TD3 to be able to solve the task accurately using roughly twice the amount of training samples. This indicates that the area around the goal in which the object is considered to be at the desired location is relatively large. If we apply a stricter criterion for the goal being reached by reducing the size of the goal area by a factor of 100, we can see that hindsight samples are necessary to learn from sparse rewards. In this variant, TD3 fails to learn a useful policy while both UVD and HER performing similarly (see Figure 2c).

The second domain in the suite, *FetchSlide*, requires the robot to slide the object toward a desired location that is out of reach of the robot arm. In Figure 2b, we can see UVD and HER learning to solve the task quickly while TD3 without hindsight samples requires significantly more training samples. Unlike in the case of *FetchPush*, TD3+UVD learns slightly faster in this domain than TD3+HER but both are able to solve the task eventually. Both, *FetchSlide* and *FetchPush*, are deterministic domains that play to the strengths of hindsight experience replay. In practice, however, manipulation with a real robot arm is always noisy. In some cases, HER can overcome this noise despite suffering from hindsight bias; however, this is not always the case. Here, we introduce a variation of the *FetchSlide* domain which adds Gaussian noise to the actions of the agent. We scale this noise based on the squared norm of the chosen actions $\frac{1}{2e} \|\max(0, a - 0.5 \cdot \mathbf{1})\|_2^2$. This scaling allows the agent to adapt to the noise; however, doing so requires the

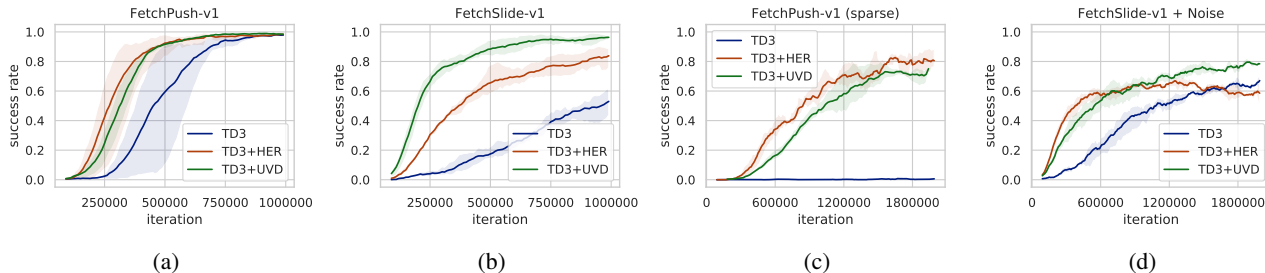


Figure 2: Comparison of TD3, UVD and HER on variations of the Fetch manipulation domains. *FetchPush* and *FetchSlide* correspond to the original domains. *FetchPush (Sparse)* shows the advantage of hindsight updates when the required precision is significantly higher while *FetchSlide + Noise* shows the effect of hindsight bias in stochastic domains.

agent to accurately assess the risks of its actions. In Figure 2d, we can see that while HER initially learns quickly as in the deterministic domain, it converges to a policy that is noticeably worse than the policy found by TD3+UVD. This shows the effect of hindsight bias: in the presence of noise, the agent assumes the noise to be benign. UVD, on the other hand, estimates the risk accurately and achieves a higher success rate than HER.

6.2. Imitation Learning

Next, we evaluate Value Density Imitation on common benchmark tasks and show that it outperforms the current state of the art. We point out issues with using these domains in an imitation learning context verbatim and introduce more difficult variations of the tasks that address those issues. The suite of simulated locomotion tasks found in OpenAI Gym (Brockman et al., 2016) has become a standard benchmark task for reinforcement learning due to their complex dynamics and proprioceptive, relatively low-dimensional state-action spaces. Recently, the suite of benchmark tasks has been used to evaluate imitation learning algorithms as well with Ho and Ermon (2016) showing GAIL to solve the tasks using only a handful of demonstrated trajectories; however, we find that the unmodified locomotion tasks, despite their popularity, are easily exploited in an imitation learning context. While it is impressive that GAIL is able to solve *Humanoid-v2* with less than a dozen of disjointed demonstrated states, it is also clear that the agent is not learning to imitate the motion itself.

The dominating source of reward in these tasks comes from the velocity in a particular direction. This is problematic as the velocity is fully observable as part of the state and, in the case of humanoid, may be encoded in more than one of the features found in the state-vector. Even the simple average of the state-features may be equivalent to a noisy version of the original reward signal. Moreover, as the reward is a linear combination of state-features, we know that accurate distribution matching is not necessary and matching feature

expectations is sufficient (Abbeel and Ng, 2004; Ho and Ermon, 2016). To alleviate this, we remove task-space velocities in x, y directions from the state-space. A second source of bias can be found in the termination condition of the locomotion domains. Kostrikov et al. (2019) point out that GAIL is biased toward longer trajectories and thus tries to avoid termination, which in the case of locomotion means to avoid falling. While Kostrikov et al. adjust the algorithm itself to avoid such bias, we instead propose to remove the termination condition and use an evaluation which cannot be exploited by a biased method. Besides removing bias, this makes the learning problem significantly more difficult as a significant portion of the agent’s experience is far from the demonstrated path.

We focus on two locomotion tasks in particular: *HalfCheetah-v2* and *Humanoid-v2*. We choose *HalfCheetah-v2* as it is comparatively easy to train an agent to move in the right direction while it is comparatively difficult to move at high speeds. With the original threshold for solving the task being set at a score of 4500, recent advances in reinforcement learning train policies that achieve 3-4 times as high a score (Fujimoto et al., 2018; Haarnoja et al., 2018) (although we find that removing velocity from the state reduces the top-speed achieved by the TD3-trained expert). Our second domain of choice is *Humanoid-v2*, which is generally considered to be the most complex locomotion task. Unlike in the *HalfCheetah-v2* domain, learning to move without falling can be a significant challenge for a learning agent. We furthermore find it sufficient to match state-distributions to solve *HalfCheetah-v2* and thus teach the agent from observation only when using VDI. In the case *Humanoid-v2*, we find that demonstrated actions significantly aid exploration and thus include them. We compare the demonstration-efficiency of Value Density Imitation with GAIL, the state-of-the-art in terms of demonstration-efficiency on these domains. Similar to Ho and Ermon (2016), we subsample each trajectory to make the problem more challenging. The results can be seen in Figures 3a and

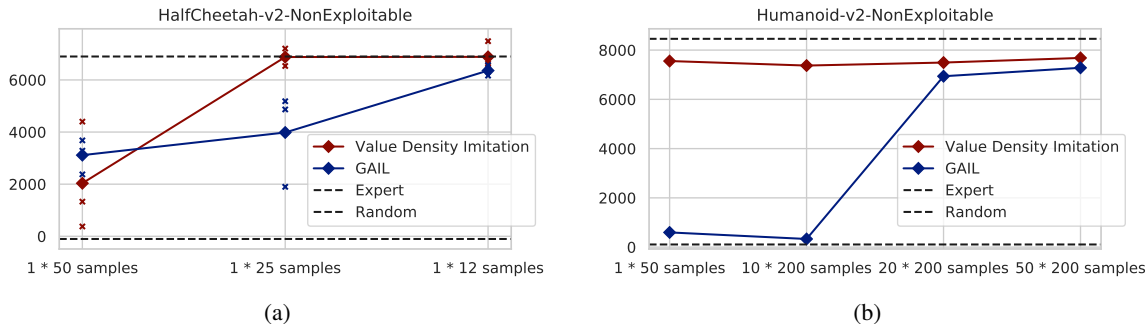


Figure 3: Comparison of GAIL and VDI on variations of standard benchmark tasks. x-axis shows the number of provided demonstration trajectories as well as the number of state-action pairs collected from each trajectory. VDI is able to outperform GAIL when the number of provided demonstrations is low.

3b. While both methods are able to achieve near-expert performance on *HalfCheetah-v2-NonExploitable* using a single demonstrated trajectory sub-sampled at the same rate as used by Ho and Ermon, we find VDI to be able to imitate the expert if the trajectory is sub-sampled even further. On *Humanoid-v2-NonExploitable*, we find the difference to be more drastic: while GAIL is able to learn locomotion behavior from a similar number of trajectories as used in the original paper (but using more state-action pairs), the performance drops off quickly if we reduce the number of trajectories further. VDI is able to imitate the expert using only a single demonstrated trajectory.

Both methods are able to achieve great demonstration-efficiency by matching the expert’s state-action distribution; however, GAIL does so by learning a distance function using demonstrations as training samples. As the number of demonstrations shrinks, learning a good discriminator to serve as a reward becomes more difficult. VDI side-steps this issue by learning a goal-conditioned Q-function based on self-supervised roll-outs alone. The demonstrations are used to condition the Q-function and don’t serve directly as training data for any network.

7. Related Work

Addressing the problem of goal-conditioned reinforcement learning, Sutton et al. (2011) introduce HORDE, the first paper to utilize recent advances in off-policy RL to learn multiple value functions simultaneously and the foundation for UVFA (Schaul et al., 2015) and HER (Andrychowicz et al., 2017) which our work heavily relies on. Recent work by Nair et al. (2018) and Sahni et al. (2019) propose approaches that adapt HER to the setting of high-dimensional, visual features. While our work is based on RealNVP which was originally invented for modeling images, learning universal value densities in such a high-dimensional setting comes with its own set of challenges, not the least of which

are computational, and is an interesting avenue for future research. To the best of our knowledge, the first paper to identify bias in HER is (Lanka and Wu, 2018); however, while the authors propose a heuristic method to handle this issue, no principled method to use hindsight samples in a completely unbiased way has been proposed to date. Most closely related to the method of Universal Value Density Estimation itself are Temporal Difference Models (Pong et al., 2018). TDMs use a squared error function as a terminal value and use bootstrapping to propagate this value over a finite horizon. F_γ can similarly be seen as a model of terminal value, where the use of it as a lower bound allows bootstrapping with an infinite time-horizon. While there are further similarities to our method when using a Gaussian density estimator, the proposed method does not address hindsight bias, TDMs do not address hindsight bias.

Value Density Imitation is closely related to other work in state-action-distribution matching such as adversarial methods. Ho and Ermon (2016) show early work in inverse reinforcement learning to be reducible to state-action distribution matching (e.g. Abbeel and Ng, 2004; Ziebart et al., 2008) and furthermore introduce GAIL. Using an adversarial objective, GAIL trains a discriminator to identify expert transitions while using reinforcement learning to train the agent to fool the discriminator. Several approaches have been introduced that build on this idea. Adversarial Inverse Reinforcement Learning uses an adversarial objective to learn a fixed reward function (Fu et al., 2018) while Discriminator Actor-Critic (Kostrikov et al., 2019) reduces the number of environment interactions required. GPRIL (Schroecker et al., 2019) attempts to match the state-action-distribution using a similar long-term generative model. In contrast to VDI, GPRIL cannot easily be combined with temporal-difference learning techniques as the model is used to generate samples and struggles with larger time-horizons as can be found in the locomotion benchmark tasks.

References

- Abbeel, P. and Ng, A. Y. (2004). Apprenticeship learning via inverse reinforcement learning. In Greiner, R. and Schuurmans, D., editors, *International Conference on Machine Learning*, pages 1–8.
- Andrychowicz, M., Wolski, F., Ray, A., Schneider, J., Fong, R., Welinder, P., McGrew, B., Tobin, J., Abbeel, O. P., and Zaremba, W. (2017). Hindsight experience replay. In *Advances in Neural Information Processing Systems*, pages 5048–5058.
- Aytar, Y., Pfaff, T., Budden, D., Paine, T., Wang, Z., and de Freitas, N. (2018). Playing hard exploration games by watching youtube. In *Advances in Neural Information Processing Systems*, pages 2930–2941.
- Brockman, G., Cheung, V., Pettersson, L., Schneider, J., Schulman, J., Tang, J., and Zaremba, W. (2016). *OpenAI Gym*.
- Dinh, L., Sohl-Dickstein, J., and Bengio, S. (2016). Density estimation using Real NVP. *arXiv preprint arXiv:1605.08803*.
- Fu, J., Luo, K., and Levine, S. (2018). Learning robust rewards with adversarial inverse reinforcement learning. In *International Conference on Learning Representations*.
- Fujimoto, S., Hoof, H., and Meger, D. (2018). Addressing function approximation error in actor-critic methods. In *International Conference on Machine Learning*, pages 1582–1591.
- Goodfellow, I., Pouget-Abadie, J., Mirza, M., Xu, B., Warde-Farley, D., Ozair, S., Courville, A., and Bengio, Y. (2014). Generative adversarial nets. In *Advances in Neural Information Processing Systems*, pages 2672–2680.
- Haarnoja, T., Zhou, A., Abbeel, P., and Levine, S. (2018). Soft actor-critic: Off-policy maximum entropy deep reinforcement learning with a stochastic actor. In *International Conference on Machine Learning*, pages 1856–1865.
- Ho, J. and Ermon, S. (2016). Generative adversarial imitation learning. In *Advances in Neural Information Processing Systems*, pages 4565–4573.
- Kingma, D. P. and Welling, M. (2014). Auto-encoding variational bayes. In *International Conference on Learning Representations*.
- Kostrikov, I., Agrawal, K. K., Dwibedi, D., Levine, S., and Tompson, J. (2019). Discriminator-actor-critic: Addressing sample inefficiency and reward bias in adversarial imitation learning. In *International Conference on Learning Representations*.
- Lanka, S. and Wu, T. (2018). ARCHER: Aggressive Rewards to Counter bias in Hindsight Experience Replay. *arXiv preprint arXiv:1809.02070*.
- Mnih, V., Kavukcuoglu, K., Silver, D., Rusu, A. A., Veness, J., Bellemare, M. G., Graves, A., Riedmiller, M., Fidjeland, A. K., Ostrovski, G., et al. (2015). Human-level control through deep reinforcement learning. *Nature*, 518(7540):529.
- Munos, R., Stepleton, T., Harutyunyan, A., and Bellemare, M. (2016). Safe and efficient off-policy reinforcement learning. In *Advances in Neural Information Processing Systems*, pages 1054–1062.
- Nair, A. V., Pong, V., Dalal, M., Bahl, S., Lin, S., and Levine, S. (2018). Visual reinforcement learning with imagined goals. In *Advances in Neural Information Processing Systems*, pages 9191–9200.
- Nota, C. and Thomas, P. S. (2019). Is the policy gradient a gradient? *arXiv preprint arXiv:1906.07073*.
- Pathak, D., Mahmoodieh, P., Luo, G., Agrawal, P., Chen, D., Shentu, Y., Shelhamer, E., Malik, J., Efros, A. A., and Darrell, T. (2018). Zero-shot visual imitation. In *International Conference on Learning Representations*.
- Peng, X. B., Abbeel, P., Levine, S., and van de Panne, M. (2018). Deepmimic: Example-guided deep reinforcement learning of physics-based character skills. *ACM Transactions on Graphics*, 37(4):143.
- Pomerleau, D. A. (1989). Alvin: An autonomous land vehicle in a neural network. In *Advances in neural information processing systems*, pages 305–313.
- Pong, V., Gu, S., Dalal, M., and Levine, S. (2018). Temporal Difference Models: Model-Free Deep RL for Model-Based Control. In *International Conference on Learning Representations*.
- Puterman, M. L. (2014). *Markov Decision Processes: Discrete Stochastic Dynamic Programming*. John Wiley & Sons.
- Reddy, S., Dragan, A. D., and Levine, S. (2019). Sgill: Imitation learning via regularized behavioral cloning. *arXiv preprint arXiv:1905.11108*.
- Ross, S., Gordon, G., and Bagnell, D. (2011). A reduction of imitation learning and structured prediction to no-regret online learning. In *Proceedings of the fourteenth international conference on artificial intelligence and statistics*, pages 627–635.
- Sahni, H., Buckley, T., Abbeel, P., and Kuzovkin, I. (2019). Visual Hindsight Experience Replay. *Advances in Neural Information Processing Systems*.

- Schaul, T., Horgan, D., Gregor, K., and Silver, D. (2015). Universal Value Function Approximators. In *International Conference on Machine Learning*, pages 1312–1320.
- Schroecker, Y. and Isbell, C. L. (2017). State Aware Imitation Learning. *Advances in Neural Information Processing Systems*, pages 2915–2924.
- Schroecker, Y., Vecerik, M., and Scholz, J. (2019). Generative predecessor models for sample-efficient imitation learning. In *International Conference on Learning Representations*.
- Silver, D., Lever, G., Heess, N., Degris, T., Wierstra, D., and Riedmiller, M. (2014). Deterministic policy gradient algorithms. In *International Conference on Machine Learning*, pages 387–395.
- Sutton, R. S., Mcallester, D., Singh, S., and Mansour, Y. (1999). Policy Gradient Methods for Reinforcement Learning with Function Approximation. *Advances in Neural Information Processing Systems*, pages 1057–1063.
- Sutton, R. S., Modayil, J., Delp, M., Degris, T., Pilarski, P. M., White, A., and Precup, D. (2011). Horde: A scalable real-time architecture for learning knowledge from unsupervised sensorimotor interaction. In *International Conference on Autonomous Agents and Multiagent Systems*, pages 761–768. International Foundation for Autonomous Agents and Multiagent Systems.
- van den Oord, A., Dieleman, S., Zen, H., Simonyan, K., Vinyals, O., Graves, A., Kalchbrenner, N., Senior, A., and Kavukcuoglu, K. (2016). Wavenet: A generative model for raw audio. *arXiv preprint arXiv:1609.03499*.
- van den Oord, A., Kalchbrenner, N., and Kavukcuoglu, K. (2016). Pixel Recurrent Neural Networks. In *International Conference on Machine Learning*, pages 1747–1756.
- van den Oord, A., Li, Y., Babuschkin, I., Simonyan, K., Vinyals, O., Kavukcuoglu, K., van den Driessche, G., Lockhart, E., Cobo, L. C., Stimberg, F., et al. (2017). Parallel wavenet: Fast high-fidelity speech synthesis. *arXiv preprint arXiv:1711.10433*.
- Wang, R., Ciliberto, C., Amadori, P. V., and Demiris, Y. (2019). Random expert distillation: Imitation learning via expert policy support estimation. In *International Conference on Machine Learning*, pages 6536–6544.
- Ziebart, B. D., Maas, A. L., Bagnell, J. A., and Dey, A. K. (2008). Maximum entropy inverse reinforcement learning. In *Aaai*, volume 8, pages 1433–1438. Chicago, IL, USA.

A. Practical considerations

There are a number of implementation decisions that were made to improve the sample-efficiency and stability of Value Density Estimation and its application to imitation learning. Here, we review these decisions in more detail.

A.1. Universal Value Density Estimation

Using an exploration policy: In most cases self-supervised roll-outs will require the agent to explore. In our method, we combine a temporal difference update rule as is usually found in deterministic policy gradients with density estimation. While the temporal-difference update rule can handle off-policy data from an exploration policy, density-estimation is on-policy. In practice, however, Fujimoto et al. (2018) add Gaussian noise to the target-Q function and report better results by learning a smoothed Q-function that is akin to the on-policy Q-function with Gaussian exploration noise. It thus stands to reason that we can omit off-policy correction in the density-estimator.

Truncating the time horizon: The training data for learning a long-term model can be fairly noisy. While we can expect density estimation to be efficient over a horizon of just a few time-steps, the variance increases dramatically as γ increases. This is the primary motivation for utilizing temporal-difference learning in conjunction with universal value density estimation. To better facilitate stable training, we truncate the time-horizon of the density-estimator to a fixed number of time-steps T . The temporal-difference learning component is thus solely responsible for propagating the value beyond this fixed horizon. The effect this has on the optimal policy is small: the Q-value will be underestimated by ignoring visitations with time-to-recurrence greater than T . A greater time-horizon boosts the effect of hindsight samples and leads to a learning signal that is less sparse while a smaller time-horizon reduces the variance of the estimator.

Using a replay buffer: Using a replay buffer is essential for sample-efficient training with model-free reinforcement- and imitation-learning methods and improves the stability of deterministic policy gradients. We find that this is true for training long-term generative models as well. While importance sampling based off-policy correction for density estimation is possible, we find that it introduces instabilities and is thus undesirable. Instead, we propose to use a separate, shorter replay-buffer for density estimation to mitigate the undesirable effects of off-policy learning while retaining some of the benefits.

Delayed density updates: Temporal-difference learning with non-linear function approximation is notoriously unstable. To help stabilize it, a common (Mnih et al., 2015;

Fujimoto et al., 2018) trick is delay the update of the target network and allow the Q-function to perform multiple steps of regression toward a fixed target. Since we use the long-term predictive model F_ω to calculate the temporal-difference regression target, we apply the same trick here. We maintain a target network $F_{\bar{\omega}}$ which we set to be equal to the online density estimator F_ω after a fixed number of iterations. In Value Density Imitation, we use the same procedure to maintain a frozen target network of the unconditional state density estimator d_ω .

Normalizing states: As our method depends on density estimation, the resulting values are heavily affected by the scale of the features. We therefore normalize our data based on the range observed in random roll-outs as well as, in the case of imitation learning, the range seen in the given demonstrations.

A.2. Value Density Imitation

Averaging logits: While the dimensionality of the goal in goal-conditioned reinforcement learning is typically small, Value Density Imitation requires us to use the entire state as a goal. This, however, can be difficult if the number of features is large. If the state-features are independent, the density suffers from the curse of dimensionality as it is multiplicative and the Q-values will be either extremely large or extremely small. Even if the true density function does not exhibit this property, Normalizing Flows predict the density as a product of N predicted logits and prediction errors are therefore multiplicative. To combat this, we take the average of the predicted logits rather than the sum, effectively taking the N -th square root of the Q-function. We find that this approximation works well in practice and justify it further in appendix B.

Bounding weights on demonstrated states: In Value Density Imitation, we sub-sample demonstration states proportional to $\frac{1}{d_\omega(\bar{s})}$ to ensure demonstration states to be visited with equal probability. In this formulation, demonstration states that are especially difficult to reach may be over-sampled by a large factor and destabilize the learning process. To counteract this, we put a bound on the weight of each demonstration state: for each batch, the weights are normalized and an upper bound is applied.

Spatial and temporal smoothing: We apply two kinds of smoothing to the learned UVFA to improve the stability of the learning algorithm. Spatial smoothing ensures that similar state-action pairs have similar value and is achieved by adding Gaussian noise to training samples of the target state when training the density estimator. Temporal smoothing ensures that the learned value does not spike too suddenly. Instead of using $F_\gamma(\bar{s})$ as a temporal difference

regression target, we use a mixture of the density estimation and the temporal-difference lower bound. Using a temporal smoothing factor λ , the full temporal difference loss is then given by:

$$L(\omega) := \left(r^g(s, a) + \gamma \bar{Q} - \tilde{Q}_\omega(s, a; g) \right)^2, \\ \bar{Q} := \lambda \tilde{Q}_{\bar{\omega}}(s, a; g) + \\ (1 - \lambda) \max \left(\tilde{Q}_{\bar{\omega}}(s, a; g), F_\Phi(g|s, a) \right)$$

B. Escaping the curse of dimensionality

In section 3, we introduced a method which uses the probability density predicted by a normalizing flow as a Q function. We showed that this density Q function is a valid Q function with a corresponding reward function that is sensible for many practical task. In this appendix, we consider the numerical properties of the universal value density estimator and propose a slight variation that is easier to handle numerically. To see the numerical challenge in using density estimators as value functions, we take a look another look at a single bijector of a RealNVP; here, the bijector $f_\omega(z) = (s_\omega(z), t_\omega(z))$ is predicting an affine transformation of $z \sim p_z(\cdot) = \mathcal{N}(0, I)$ to $x \sim p_x(\cdot)$, i.e. $x_i = s_\omega(z)_i z_i + t_\omega(z)_i$. The log-density of x is then given

as $p_x(x) = e^{\sum_{i=0}^N s_\omega^{-1}(x) - \left(\frac{x_i - t_\omega^{-1}(x)_i}{s_\omega^{-1}(x)_i} \right)^2 + \log \frac{1}{\sqrt{2\pi}}}$. It is readily apparent that this value can easily explode, especially when used as a target Q value in the mean-squared loss of a temporal difference update. To combat this, we propose to scale the logits with the dimensionality N , i.e. we use $p_x(x) = e^{\frac{1}{N} \sum_{i=0}^N s_\omega^{-1}(x) - \left(\frac{x_i - t_\omega^{-1}(x)_i}{s_\omega^{-1}(x)_i} \right)^2 + \log \frac{1}{\sqrt{2\pi}}}$. As this corresponds to only a constant factor on $\log F_\gamma$, the gradient-based density estimation is not affected.

While the change is simple, average logits instead of taking the sum, we need to justify the approximation anywhere the value density and the Q-function are used: first, we show that $J(\theta)^{\frac{1}{N}}$ can be used in place of $J(\theta)$ in both, goal-conditioned reinforcement learning and in imitation learning without changing the optimal policy; second, we justify using $Q_{r,g}^{\mu_\theta}(s, a)^{\frac{1}{N}}$ in place of $Q_{r,g}^{\mu_\theta}(s, a)$ when computing the policy gradient; and, finally, we show that we can justify the use of the N-th root in the temporal difference learning update.

Using the scaled objective $J(\theta)^{\frac{1}{N}}$: Here, we have to consider two cases. In the case of goal-conditioned RL, we have to show that $\max_\theta J(\theta) = \max_\theta J(\theta)^{\frac{1}{N}}$. To this end, it is sufficient to note that the reward function is strictly non-negative and thus $(\cdot)^{\frac{1}{N}}$ is a monotonous function. In the case of imitation learning, we can immediately see that the change corresponds to a constant factor on the state-

distribution gradient:

$$\frac{1}{N} \nabla_{\theta} \log d^{\mu_{\theta}}(\bar{s}) = \frac{\nabla_{\theta} J_{r^{\bar{s}}}(\theta)^{\frac{1}{N}}}{d^{\mu_{\theta}}(\bar{s})^{\frac{1}{N}}} \quad (9)$$

Estimating the policy gradient $\nabla_{\theta} J(\theta)^{\frac{1}{N}}$: The deterministic policy gradient theorem (Silver et al., 2014) shows that maximizing the Q-value in states sampled from the agent’s discounted on-policy state-distribution is equivalent to maximizing the reinforcement-learning objective. This is immediately apparent if the representation of the policy is sufficiently expressive and agent is able to take the action with maximum value in every state. Due to monotonicity of $(\cdot)^{\frac{1}{N}}$, this is true when using $Q_{\Phi}(s, a; g)^{\frac{1}{N}}$ as well. If the policy is not able to maximize the Q-function everywhere, the deterministic policy gradient theorem shows that sampling from the discounted state-distribution leads to the agent making the right trade-offs. Using $Q(s, a; g)^{\frac{1}{N}}$, however, leads to a different trade-off. In practice, this is typically ignored: deterministic policy gradients used off-policy with a replay-buffer are not guaranteed to make the right trade-off and even if they are used on-policy, the discount-factor is typically ignored and the resulting estimate of the policy gradient is biased (Nota and Thomas, 2019).

$Q_g^{\mu}(s, a)^{\frac{1}{N}}$ as TD target: Finally, we need to show that we can use the N-th root in the computation of the temporal difference learning target. To this end, we make use of the fact that the reward in continuous environments can be assumed to be 0 when computing the temporal difference target. In this case $(r^g(s, a) + \gamma Q_{r^g}^{\mu}(s', \mu(s')))^{\frac{1}{N}}$ becomes $\gamma^{\frac{1}{N}} Q_{r^g}^{\mu}(s', \mu(s'))^{\frac{1}{N}}$ and increasing γ is sufficient to compute a valid regression target for $Q_{r^g}^{\mu}(s, a)^{\frac{1}{N}}$

C. Hyperparameters

In Table 1, we list the hyper-parameters used for TD3, TD3+HER and TD3+UVD on the Fetch experiments. When applicable, we largely use the same hyper-parameters for each algorithm. Two important exceptions are the learning rate which is tuned individually for each algorithm (TD3+UVD benefits reliably from higher learning rates whereas TD3 and TD3+HER does not always converge to a good solution at higher learning rates) as well as the output activation of the Q-network. A tanh activation is used to scale the value to the range of -50 to 50 in the case of TD3 and TD3+HER as we found this to drastically improve performance. Since the density is not bounded from above, the same activation cannot be used in the case of TD3+UVD.

In Table 2, we list the hyper-parameters used for VDI in the locomotion experiments. Parameters are largely identical between environments; however, in some cases we trade off higher learning speed for reduced accuracy on *HalfCheetah*.

In the case of GAIL, we use the implementation found in OpenAI baselines⁴, using 16 parallel processes (collecting 16 trajectories per iteration) and do not modify the parameters.

⁴<https://github.com/openai/baselines/tree/master/baselines/gail>

| General parameters | |
|---|---|
| Environment steps per iteration | 1 |
| γ | 0.98 |
| Batch size | 512 |
| Replay memory size | 1500000 |
| Short replay memory size | 50000 |
| Sequence Truncation (Density estimation training) | 4 |
| Optimizer | Adam |
| Policy | |
| Hidden layers | 400, 400 |
| Hidden activation | leaky relu |
| Output activation | tanh |
| Exploration noise σ | 0.1 |
| Target action noise σ | 0.0 |
| Learning rate | $2 \cdot 10^{-4}$ (TD3, TD3+HER), $8 \cdot 10^{-4}$ (TD3+UVD) |
| Q-network | |
| Hidden layers | 400, 400 |
| Hidden activation | leaky relu |
| Output activation | 50 tanh (TD3, TD3+HER), linear (TD3+UVD) |
| Learning rate | $2 \cdot 10^{-4}$ (TD3, TD3+HER), $8 \cdot 10^{-4}$ (TD3+UVD) |
| RealNVP | |
| Bijector hidden layers | 300, 300 |
| Hidden activation | leaky relu |
| Output activation, scale | tanh(log()) |
| Output activation, translate | linear |
| num bijectors | 5 (slide), 6 (push) |
| Learning rate | $2 \cdot 10^{-4}$ |

Table 1: Common parameters in Fetch environments

| Parameter | <i>HalfCheetah</i> | <i>Humanoid</i> |
|---|--|-------------------|
| General parameters | | |
| Environment steps per iteration | 10 | 10 |
| γ | 0.995 | 0.995 |
| Batch size | 256 | 256 |
| Replay memory size | 1500000 | 1500000 |
| Short replay memory size | 500000 | 500000 |
| Sequence Truncation (Density estimation training) | 4 | 4 |
| Optimizer | Adam | Adam |
| Policy | | |
| Hidden layers | 400, 300 | 400, 300 |
| Hidden activation | leaky relu | leaky relu |
| Output activation | tanh | tanh |
| Exploration noise σ | 0.3 (until iteration 25000), 0.1 (after) | 0.1 |
| Target action noise σ | 0.0 | 0.0 |
| Learning rate | $3 \cdot 10^{-4}$ | $3 \cdot 10^{-4}$ |
| Q-network | | |
| Hidden layers | 400, 400 | 400, 400 |
| Hidden activation | leaky relu | leaky relu |
| Output activation | linear | linear |
| Learning rate | $3 \cdot 10^{-4}$ | $1 \cdot 10^{-4}$ |
| RealNVP | | |
| Bijector hidden layers | 400, 400 | 400, 400 |
| Hidden activation | leaky relu | leaky relu |
| Output activation, scale | tanh(log()) | tanh(log()) |
| Output activation, translate | linear | linear |
| num bijectors | 5 | 5 |
| Learning rate | $1 \cdot 10^{-4}$ | $2 \cdot 10^{-5}$ |
| L2-regularization | $1 \cdot 10^{-5}$ | $1 \cdot 10^{-6}$ |
| Spatial smoothing | 0.1 | 0.1 |
| Temporal smoothing | 0. | 0.98 |

Table 2: VDI parameters in locomotion environments